Vol. 22, No. 1(2023) Alim2965
Revista Mexicana de Ingeniería Química

Influence of power density and geometry of young cactus cladodes (*Opuntia ficus-indica* (L.) Mill.) on intermittent microwave drying kinetics

Influencia de la densidad energética y geometría de cladodios jóvenes de nopal (*Opuntia ficus-indica* (L.) Mill.) sobre las cinéticas de secado intermitente con microondas

T. Espinosa-Solares[1], R. Domínguez-Puerto[2*]
[1]*Departamento de Ingeniería Agroindustrial, Universidad Autónoma Chapingo, Carretera México-Texcoco km 38.5, Texcoco, Estado de México, C. P. 56230, México.*
[2]*Laboratorio de Productos Naturales. Departamento de Preparatoria Agrícola, Universidad Autónoma Chapingo, Carretera México-Texcoco km 38.5, Texcoco, Estado de México, C. P. 56230, México.*
Received: September 21, 2022; Accepted: December 6, 2022

Abstract
Due to its multiple uses, the production and consumption of nopal have increased worldwide in recent years. The influence of power density (60.3 to 538.9 W g_{db}^{-1}) on the intermittent microwave drying of young cladodes, of different sizes, was studied. In general, all drying treatments showed a sigmoid shape and three drying periods: heating (I), constant rate (II) and falling rate (III). Empirical models were used to model drying kinetics. However, although they had a good fit (R^2 from 0.965-0.998) they do not exactly represent the changes between drying periods. According to microstructural analysis of dried samples, the water was transferred from the inside to the surface of the cladode by the sides, where there is no cuticle o epidermis (which was removed by the thorn quitting process). It was determined that the drying rate in period II depends exclusively on the power density applied and not on the cladode's geometry. However, in period III the data of effective diffusivity (D_{eff}, 2.20×10^{-6} to 5.59×10^{-5} m ^{2} s^{-1}) showed that the drying rate is affected by the size and thickness of cladodes.
Keywords: Microwave intermittent drying, Cactus cladodes drying, Effective diffusion coefficient, Drying periods, Activation energy.

Resumen
Debido a sus múltiples usos, la producción y consumo del nopal ha incrementado mundialmente en los últimos años. La influencia de la densidad energética (60.3 to 538.9 W g_{db}^{-1}) sobre el secado con microondas de cladodios jóvenes y a diferentes tamaños fue estudiado. En general, todos los tratamientos mostraron tres periodos de secado: calentamiento (I), velocidad constante (II) y velocidad decreciente (III). Se usaron modelos empíricos para modelar las cinéticas de secado. Sin embargo, aunque mostraron buen ajuste (R^2 from 0.965-0.998), no representaron exactamente los cambios entre los periodos de secado. De acuerdo con la evidencia estructural, el agua migra de adentro hacía afuera del cladodio por las orillas, donde no hay cutícula (removida en el proceso de desespinado). Se determinó que, en el periodo II, la velocidad de secado depende exclusivamente de la densidad energética aplicada, no de la geometría. Sin embargo, en el periodo III, los datos obtenidos de la difusividad efectiva (D_{eff}, 2.20×10^{-6} to 5.59×10^{-5} m ^{2} s^{-1}) muestran que la velocidad de secado es afectada por el tamaño y grosor de los cladodios.
Palabras clave: Secado intermitente con microondas, Secado de cladodios de nopal, Coeficiente de difusividad efectiva, Periodos de secado, Energía de activación.

* *Corresponding author. E-mail*: rdominguezp@chapingo.mx
https://doi.org/10.24275/rmiq/Alim2965
ISSN:1665-2738, *issn-e*: 2395-8472

1 Introduction

Opuntia ficus-indica (L.) Mill. is a cactus endemic to America. It is the most popular and consumed species in México (López, de Ita, & Vaca, 2009). The leaves of the plant or cladodes are ovoid or racket-shaped (Barba *et al*., 2020), and are consumed as vegetables (Ventura-Aguilar, Bosquez-Molina, Bautista-Baños, & Rivera-Cabrera, 2017) with thorns removed and peeled; raw or cooked and are commonly called "nopales" or "nopalitos".

Nopal cladodes have been reported to contain antioxidant compounds such as phenolic acids, flavonoids, tocopherols, and vitamin C (Aruwa, Amoo, & Kudanga, 2018; Barba *et al*., 2020). Contain proteins in a range of 6.7-11.73% (Perucini-Avendaño *et al*., 2021), with a major amino acid profile such as glutamine, leucine, lysine, valine, arginine, phenylalanine, and isoleucine. Also, the presence of taurine in trace amounts has been reported (El-Mostafa *et al*., 2014). Nopal has been reported as a source of bioactive compounds for nutrition (Ventura-Aguilar *et al*., 2017), improving or protecting health, and treating diseases (El-Mostafa *et al*., 2014). Because it is a plant food, it contains a lower caloric density than other foods, and it is a source of fiber. (Aruwa *et al*., 2018), potassium and calcium (El-Mostafa *et al*., 2014).

Mexico is the largest consumer (per capita consumption of 6.4 kg (SADER, 2020) and grower of nopal in the world (44% of world production) (Ramadan, Moussa Ayoub, & Rohn, 2021). The annual production of nopalitos in 2020 in Mexico was 8.63×10^5 tons equivalent to a production value of approximately 102 million dollars (SIAP, 2021). Due to its multiple uses, the production and consumption of nopal has increased worldwide in recent years (Torres Salcido & Cornejo Oviedo, 2018).

In Mexico, nopal is produced all year round. However, in the warmer months (March to June) there is overproduction of which it estimates a loss of up to 60% (Sáenz & Berger, 2006). Consequently, it is necessary to implement post-harvest technologies to extend their shelf life (Ventura-Aguilar *et al*., 2017). One preservation method for taking advantage of nopal cladode is drying. The main advantages of drying are a decrease in feedstuff moisture and transport costs, inhibition of the growth of microorganisms, reduction of enzymatic and chemical reactions, and increased shelf life among others. In the literature, a different method of drying on cladodes has been reported: osmotic-convective (Medina-Torres, Gallegos-Infante, Gonzalez-Laredo, & Rocha-Guzman, 2008), forced convection tunnel (López *et al*., 2009), infrared drying (Touil, Chemkhi, & Zagrouba, 2014), convective transversal flow (Díaz-Ayala, Álvarez-García, & Simá-Moo, 2015), forced air circulation (Pereira *et al*., 2017), convective-vacuum (Dey *et al*., 2019). These studies have presented good results for considering drying as an appropriate method to preserve or transform cactus cladode.

Microwave drying has been widely used to reduce the water content in fruits, vegetables (Chandrasekaran, Ramanathan, & Basak, 2013) and agricultural foodstuffs (Dai *et al*., 2019). Some advantages of microwave drying are faster heating and drying time, energy savings, instantaneous and precise electronic control, reduction of waste during the process (Rattanadecho & Makul, 2016), etc.

In the open literature, works on cactus cladode microwaves drying are very limited. Our research team has reported the influence of only two power densities on equilibrium isotherms. Thus, based on the above, the objective of this article was to elucidate the influence of energy density and geometry of young cladodes of nopal (*Opuntia ficus-indica* (L.) Mill.) on intermittent microwave drying. To this end, a series of experimental techniques were used to, firstly, differentiate the drying rate periods and evaluate the influence of these effects on the mass transfer properties of the process accordingly.

2 Materials and methods

2.1 Raw material (*Opuntia ficus-indica L. (Mill.)*)

The young cladodes of fresh nopal (45 to 60 days) were purchased in the local market (Texcoco, State of Mexico), cropped from of Otumba de Gómez Farías municipality, State of Mexico. The cladodes were stored in a refrigerator at 4.0 °C ± 0.5 °C; the thorns were removed, and geometry was obtained manually by cutting with a knife until samples were subjected to the drying process to avoid their dehydration. In the process of thorn removal, sides of cladodes were quitted, which is where most of the thorns are concentrated (Fig. 1a and 1b). The cladodes were ground to guarantee homogeneity, and immediately, the moisture content was determined in thermobalance (Model No LSC60, Wiggenhauser).

2.2 Cladode geometry

By nature, cactus cladodes have a longitudinally uneven thickness and have a much smaller apical than the basal thickness (Figure 1a); in general, this difference in thickness increases with the size and age of the nopal. To reach a uniform thickness, basal part of the cladode was discarded. Slabs with circular shape were obtained (Figure 1b). Each cladode was cut to a specific weight, however, the diameter of each sample varied depending on age of each cladode. The diameter, basal and apical thickness of samples were measured using a vernier caliper.

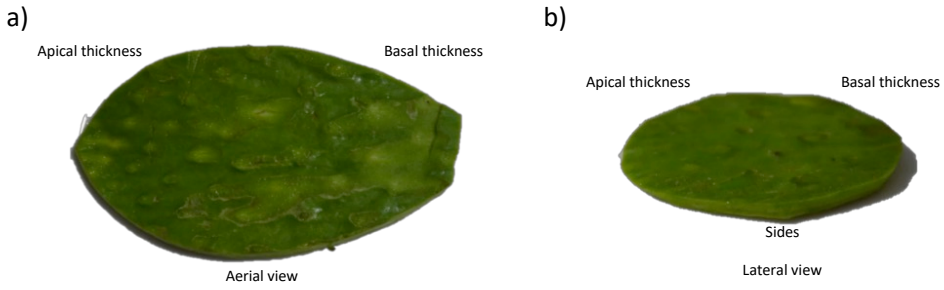

Figure 1. Cladode's shape obtained after thorn quitting (a) and after homogenization cutting process (b).

2.3 Microwave power

Drying was carried out using a microwave oven (LG, Model Ms_ 1446SQP, 37x36 x23 cm). The microwave power was determined by heating distilled water using Equation 1:

$$P = \frac{(m_1 + m_2)Cp_{H2O}\Delta T + m_2\lambda}{t_{on}} \quad (1)$$

Where P is the power of microwave (W), m_1 and m_2 (g) are the mass of heated and evaporated water respectively, Cp_{H2O} is the heat capacity of water (4.186 J °C^{-1} g_{H2O}^{-1}), ΔT is the increase in temperature before and after treatment (°C), λ is the heat of vaporization of water (2260 J g_{H2O}^{-1}) and t_{on} is the time of microwave heating (10 s).

2.4 Drying kinetics

Three power levels (217, 653 and 970 W) were established with three cladode weight levels (30, 45 and 60 g of fresh cladode), resulting in 9 treatments with different power densities (60.3, 80.4, 120.6, 181.4, 241.9, 264.4, 359.3, 362.8, 538.9 W g_{db}^{-1}). Microwave drying experiments were conducted intermittently at a pulse ratio (PR) of 0.5, according to Equation 2 (Dehghannya, Bozorghi, & Heshmati, 2018).

$$PR = \frac{t_{on} + t_{off}}{t_{on}} \quad (2)$$

Where t_{on} and t_{off} are the treatment time and without treatment respectively. The criterion for end of drying was when the weight of the cladode did not vary 0.1 g in 90s of drying or when the superficial temperature exceeded 105 °C. Water activity (a_w) value was determined at the end of drying (Aqualab Model Series 3TE).

At t_{off}, the surface temperature (FLUKE 501, Grainger) and the weight of each sample were determined. Each drying kinetic and measurement was conducted with three replications; mean values were reported with corresponding standard deviation. The moisture content was determined by Equation 3 (Siebert, Gall, Karbstein, & Gaukel, 2018):

$$M_t = \frac{m_{wb} - m_{db}}{m_{db}} \quad (3)$$

Where M_t is the moisture content (g_{H2O} g_{db}^{-1}) at time t, m_{db} is the mass of sample in dry basis (g_{db}) and m_{wb} is the mass of the cladode (g_{wb}) at time respectively.

The moisture ratio (MR) can be determined in a simplified form with Equation 4 (Karimi, Layeghinia, & Abbasi, 2021):

$$MR = \frac{M_t}{M_0} \quad (4)$$

Where M_t and M_0 indicate the moisture content at the time t and initial time of the sample (t_0).

The drying rate (DR, g_{H2O} g g_{db}^{-1} s^{-1}) was determined using Equation (5) (Jebri, Desmorieux, Maaloul, Saadaoui, & Romdhane, 2019):

$$DR = \frac{\Delta M_t}{\Delta t} \quad (5)$$

Where ΔM_t (g_{H2O} g_{db}^{-1}) is the change in moisture during the drying treatment period (ΔT, s).

2.5 Determination of drying periods

To determine the different drying phases and the critical moisture (M_{cr}), of the dataset from each drying kinetics, the period with a constant drying rate was identified visually (the value of M_t is adjusted to a straight line). Subsequently, the extremes of kinetic (heating and falling drying rate periods respectively) that did not correspond to this behavior were eliminated. To that dataset was fitted a second-degree polynomial equation (Equation 6). So, if the value of the parameter k_1, showed to be statistically significant (<95%); points were removed from one or both extremes of the dataset and allowed to adjust Equation 6. The procedure ends when k_1 ceases to be significant and the quadratic term can be disregarded to be simplified to the straight-line equation (Equation 7).

$$M_t = M_{0,cr} + k_c t + k_1 t^2 \quad (6)$$

$$M_t = M_{0,cr} + k_c t \quad (7)$$

Where $M_{0,cr}$ is the moisture where the constant drying rate period begins (and the heating period ends), k_c is the constant drying rate in this period (g_{H2O} g_{db}^{-1} s^{-1}) (Zielinska, Zielinska, & Markowski, 2018), t is the drying time and k_1 is the quadratic constant of the model.

Table 1. Fitting equations applied to intermittent microwave drying of nopal cladodes curves.

Name	Fitting equation	Reference
Page	$MR = \exp(-kt^n)$	Çinkir & Süfer (2020)
Sigmoid	$MR = a + \frac{b}{1+\exp(k(t-c))}$	Çinkir & Süfer (2020)
Rational	$MR = \frac{a+bt}{1+ct+dt^2}$	Çinkir & Süfer (2020)

By determining the constant drying rate period, $t_{0.cr}$ and t_{cr} are obtained, the time when the period of constant drying rate begins and ends. M_{cr} is obtained by substituting t_{cr} in Equation 7 and this is the point at the falling rate drying period starts.

For model the falling rate drying period, two models were used. The first is the empirical equation of Henderson and Pabis (Zielinska *et al*., 2018):

$$M_{t,dec} = M_{cr}\exp(-k_{dec}t) \tag{8}$$

Where $M_{t,dec}$ is the moisture in the falling drying rate period and k_{dec} is the drying rate (s^{-1}). This equation does not consider the geometry of the cladode.

The second model used was solution of the Fick's second law of diffusion (Eq. 9) to obtain effective diffusivity (D_{eff}, m^2 s^{-1}), a parameter used to describe drying in agricultural products (Demiray, Seker, & Tulek, 2017). Thus, Equation 9 represents the effective diffusivity of moisture in an infinite slab and supposed uniform initial moisture distribution, negligible external resistance, constant diffusivity, and negligible shrinkage (Zhu & Shen, 2014):

$$MR_{dec} = \frac{8}{\pi^2}\sum_{n=1}^{\infty}\frac{1}{(2n-1)^2}\exp\left(-\frac{(2n-1)^2\pi^2 D_{eff}t}{4L^2}\right) \tag{9}$$

Where MR_{dec} is the moisture ratio in the decreasing period, L (m) is half the thickness of the slab before the drying process.

For very large drying times, Equation 9 can be simplified and linearized by applying a natural logarithm that produces Equation 10 (Azimi-Nejadian & Hoseini, 2019):

$$\ln(MR_{dec}) = \ln\left(\frac{8}{\pi^2}\right) - \left(\frac{\pi^2 D_{eff}t}{4L^2}\right) \tag{10}$$

The slope is determined by plotting ln (MR_{dec}) against t according to the Eq. 10 (Zhu & Shen, 2014):

$$slope = \frac{\pi^2 D_{eff}}{4L^2} \tag{11}$$

The activation energy during the microwave drying process can be estimated by the modified Arrhenius equation, which was proposed by Dadali and Özbek (2008):

$$D_{eff} = D_0\exp\left(-\frac{E_a m_f}{P}\right) \tag{12}$$

Where D_0 is the preexponential factor (m^2 s^{-1}), E_a is the activation energy (W g^{-1}), m_f is the fresh mass of the sample before treatment (g), P is the microwave output power (W). E_a is obtained by linearizing Equation 12 by applying natural logarithm on both sides of the equation, producing Equation 13:

$$\ln(D_{eff}) = \ln(D_0) - \left(\frac{E_a m_f}{P}\right) \tag{13}$$

E_a is the slope resulting from plotting $\ln(D_{eff})$ vs m_f P^{-1} (g W^{-1}).

2.6 *Modeling drying kinetics with fitting equations*

The complete experimental data from each treatment were adjusted to 20 equations available in the literature. However, only three (Table 1) were able to replicate the sigmoidal behavior presented by the experimental drying curves. The fitting was made using Sigmaplot 14.0 software (Systat Software Inc., 2017); it was evaluated using three statistical parameters: the coefficient of determination (R^2), chi square (χ^2, Equation 14) and root of the mean square error (RMSE, Equation 15) (Briki, Zitouni, Bechaa, & Amiali, 2019):

$$RMSE = \left[\frac{1}{N}\sum_{i=1}^{N}(MR_{exp,i} - MR_{pre-i})^2\right]^{1/2} \tag{14}$$

$$\chi^2 = \frac{\sum_{i=1}^{N}(MR_{exp,i} - MR_{pre,i})^2}{N-z} \tag{15}$$

Where $MR_{exp,i}$ and $MR_{pre,i}$ with experimental moisture ratio observed and predicted over time ith, N is the number of observations and z is the number of constants of each model.

2.7 *Cladode microstructure by scanning electron microscopy (SEM)*

The microstructures of samples of freeze-dried cladodes and microwave drying (at 60.3 and 538.9 W g_{db}^{-1}) were observed to analyze the structural impact of each treatment. The observation was made using a scanning electron microscope (JSM-6390 LV, JEOL, Japan) equipped with an energy dispersive X-ray (EDS) detector and a Peltier cooling stage. Dried cladodes samples were mounted on brass sample holders using double-sided carbon tape and coated with gold under vacuum sputtering (Desk IV, Denton Vacuum). The equipment was operated using an acceleration voltage of 20kV and the images were obtained at different magnifications.

Table 2. Physical characteristics of fresh cactus cladodes slabs.

Treatment (#)	Power density (W g_{db}^{-1})	Apical thickness (mm)	Basal thickness (mm)	Average thickness (mm)	Diameter (mm)
1	60.3	4.33±0.47	8.33±0.47	6.3±0.33	126.7±16.1
2	80.4	4.00±0.00	8.00±0.00	6.0±0.00	113.3± 5.8
3	120.6	4.00±0.00	6.33±0.47	5.2±0.24	80.0± 5.0
4	181.4	4.50±0.50	8.50±0.50	6.5±0.35	123.3±7.6
5	241.9	4.67±0.47	6.67±0.47	5.7±0.33	116.7±11.5
6	269.4	5.00±0.00	9.00±0.82	7.0±0.41	128.3±7.6
7	359.3	4.00±0.00	8.50±0.50	6.3±0.25	107.5±3.5
8	362.8	4.00±0.00	8.00±0.00	6.0±0.00	80.0± 0.0
9	538.9	4.00±0.82	6.67±0.47	5.3±0.47	83.3± 2.9

3 Results and discussion

3.1 Characteristics of cladode

On average the moisture of fresh cladode was 14.3 ± 0.39 g_{H2O} g_{db}^{-1} (93.85±0.43 %). The moisture content for nopal has been reported within this range (Cruz-de la Cruz, Espinosa-Solares, Aguilar-Méndez, Guerra-Ramírez, & Hernández-Eugenio, 2020; Dey *et al*., 2019; Quintero-García *et al*., 2021). Table 2 shows the apical, basal, and average thickness of the cladodes before being subjected to the drying process. It can be observed that the thickness is not uniform; the basal thickness is larger than the apical. It can also be observed that longer cladodes have a greater apical thickness. This may be due to the vegetal morphology of the cladode because basal part or neck of the cladode supports all the weight.

3.2 Structural analysis

Figure 2 shows the images of the structure of the cladode cuticle of lyophilized nopal (a), used as a control group for comparison, and microwaved drying at the power densities of 60.3 (b) and 538.9 W g_{db}^{-1}(c). In all treatments, white granules were observed that are probably oxalate crystals. These crystals have already been reported in microwave-dried nopal cladodes (Cruz-de la Cruz *et al*., 2020) and hot air (Quintero-García *et al*., 2021). The presence of these small crystals on the surface can be caused by the transport of mucilage, which occurs from the inside to the outside, during the drying process.

The lyophilized sample showed open channels or pores throughout the cuticle (Figure 2a). In addition, no shrinkage is observed. The pores can be caused by the expansion of water when it becomes steam, due to the vacuum to which the sample is subjected during freeze-drying. When vacuum drying is applied, the porosity in the plant material increases and decreases shrinkage. This porosity was observed in Cherry Laurel Fruit dried with ultrasound-assisted vacuum drying (USV), and freeze-drying (Turkmen, Karasu, & Karadag, 2020) and orange peel using microwave vacuum drying (MVD) (Shu *et al*., 2020). On the other hand, the microwave-dried samples (Figure 2b and 2c) presented eruptions on the cuticular surface, no channels or pores were observed and there was shrinkage. Cuticular eruptions match with some stomata that can show and protrude on the surface. Eruptions that do not match the stomata can be druses (oxalate crystals, under the epidermis of the nopal), which do not suffer shrinkage. The sample subjected to a lower power density (60.3 W g_{db}^{-1}) presented more smooth-rounded cuticular eruptions (Figure 2b) and grooves or subcuticular channels with a softer or rounded shape; while in the sample subjected to 538.9 W g_{db}^{-1} (Figure 2c) it was observed that the eruptions are less smooth-edged, and the grooves are straight. This can be caused because at a higher energy density the water vapor migrates faster to the surface and with greater energy which does not allow the cladode to recover its shape and structure. In microwave drying of turmeric slices (Surendhar, Sivasubramanian, Vidhyeswari, & Deepanraj, 2019) this phenomenon was observed; with a greater power density the size of the pores or channels increases and the number of these in the plant structure decreases. In addition, in this research work, microwave-dried samples, no output is observed in the channels, nor are pores visible on the cuticle (Figure 2b and 2c). The structure's appearance suggests that the water was sucked from the inside, which explains the grooved structure and cuticular eruptions. A similar phenomenon was observed in the drying of orange peels with vacuum microwave drying by applying different vacuum levels (Dong *et al*., 2021). In that work it was showed the outer structure of the orange peel presented gaps or holes on the surface, as the vacuum level increased, the holes presented greater depth. In cross-sections, pores or channels with outlets were observed. The outer structure of the orange peel is much harder than the inner one, so the water will come out where there is less resistance.

Our research group has reported that in microwave-dried nopal cladodes nopal no channels or pores are observed on the surface. However, in the cross-sections the formation of channels with large openings can be observed (Cruz-de la Cruz *et al*., 2020), which agrees with the results in the present work.

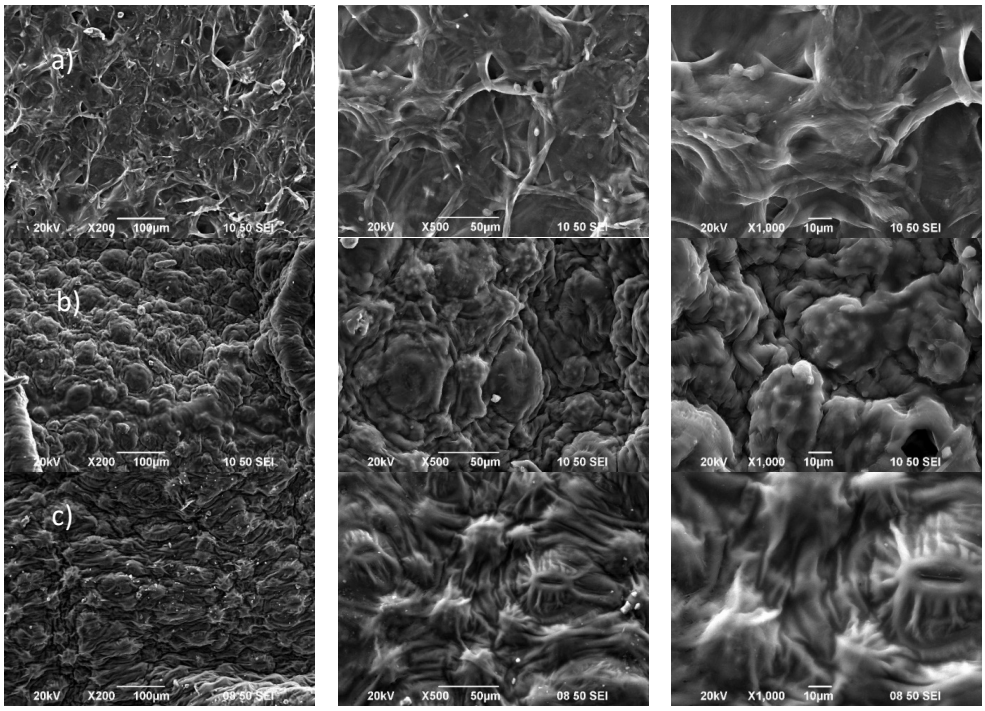

Figure 2. Microstructure of cladode's cuticle at different treatments. Row 1 (a): Liophilized, row 2 (b): 60.3 W g_{db}^{-1}, row 3 (c): 538 W g_{db}^{-1} at 200, 500 and 1000x respectively.

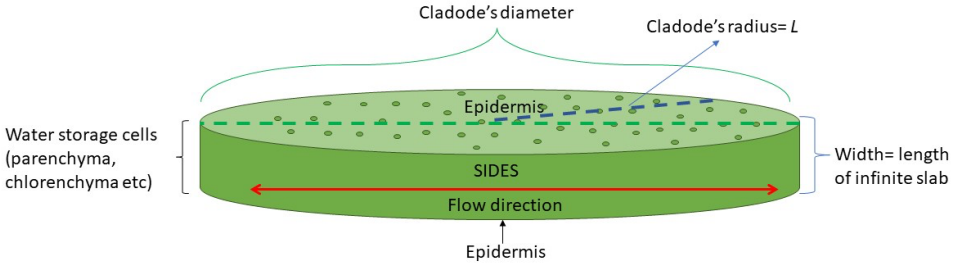

Figure 3. Schematic dimension and consideration of cactus cladode's sample for modelling the diffusion of water

This suggests that the water comes out of the cladodes' lateral cuts (or sides) and not through the cuticle. The cladode cuticle is formed by a relatively thick waxy layer whose function is to retain water within the cladode (Barba *et al*., 2020; Inglese, Mondragon Jacobo, Nefzaoui, & Sáenz, 2018; Ventura-Aguilar *et al*., 2017). By removing the edges in the thorn quitting process, mucilaginous cells such as parenchyma, chlorenchyma, and vascular and nuclear tissue are exposed (Perucini-Avendaño *et al*., 2021). López *et al*. (2009) reported that in the thorn quitting process, about 30% of the cuticle that covers the nopal is removed; this leaded a reduction of drying time (between 46 and 60%) for convective drying at 45 and 60 °C. According to the evidence found, it can be suggested that in microwave drying of cladode, water migrates to the outside by the sides of the cladode because it presents lower resistance compared to the upper and lower cuticle that which basically impermeable. Based on the structural evidence, in Equation 9, L value is the radius of each sample of cladode. Figure 3 shows the model of diffusion.

3.3 Drying periods

Figures 4, 5 and 6 show the drying kinetics for all treatments. Each one shows behavior of MR, superficial temperature, and DR. All treatments showed three drying periods: heating (period I), constant drying rate (period II) and falling rate (period III). In the plots, each period is delimited with dotted blue lines. The period with constant drying was delimited according to the proposed method (section 2.4); thus, the right and left extremes corresponded to heating and falling rate periods. These three drying periods have been reported

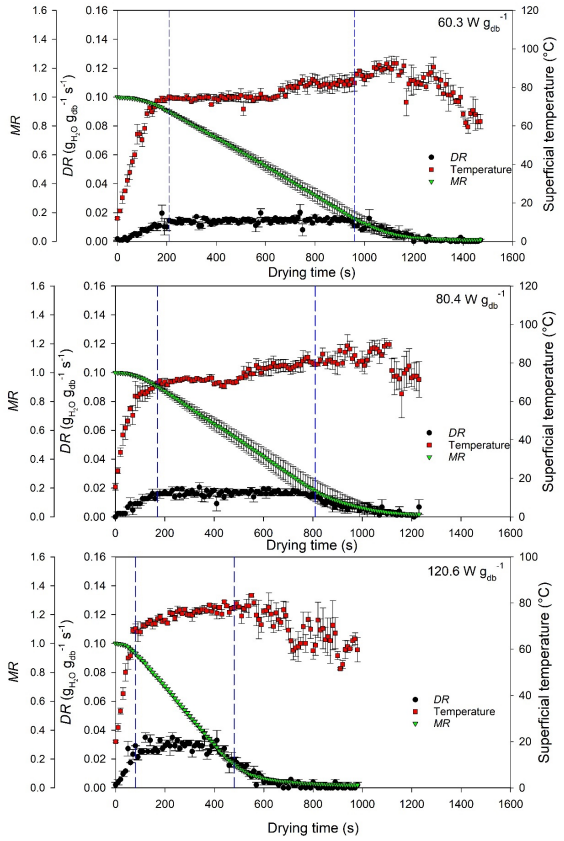

Figure 4. Drying curves of cactus cladodes at 60.3, 80.4 and 120.6 W g_{db}^{-1}.

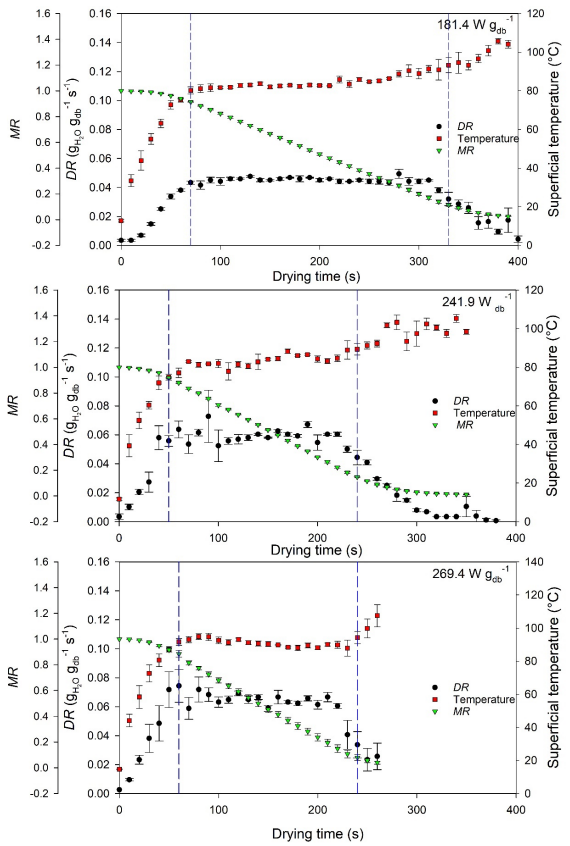

Figure 5. Drying curves of cactus cladodes at 181.4, 241.9 and 269.4 W g_{db}^{-1}.

in the literature for drying potato chips with microwave multiflash (Barreto, Tribuzi, Marsaioli Junior, Carciofi, & Laurindo, 2019), intermittent microwave drying of apple slices (Liu, Grimi, Lebovka, & Vorobiev, 2019); sweet potato slices with vacuum microwave drying (Monteiro, Gomide, Link, Carciofi, & Laurindo, 2020), and carambola slices with solar drying (García-Valladares *et al*., 2022).

In general, the total drying time, and the length of the period I and II decreased with the increase in energy density. On average the critical and residual moisture of the treatments were 2.4 ± 0.49 and 0.43±0.30 g_{H2O} g_{db}^{-1} respectively. The final value of a_w was below 0.6 for all treatments (Table 3), except for treatment 269.4 W g_{bd}^{-1}. This treatment showed a higher M_f than the others; this because the drying had to stop by the limit temperature reached. A value of a_w less than the range 0.7-0.6 ensures that the food can be preserved for longer (Shafiur-Rahman, 2020).

The drying rate in period II is directly proportional to the applied energy density (Figures 4-6); this is confirmed by the trend obtained by plotting obtained -k_c value (Equation 7) for each treatment (Table 4), since the trend is adjusted to a straight line (R^2=0.9891). In this period, the drying rate is highly dependent on the applied energy density and is not affected by the geometry of the cladode. A maximum drying rate was not reached in the evaluated interval of power densities. It is necessary to explore higher power densities to achieve a higher drying rate in less time. In this period the drying rate is highly dependent on the applied energy density, and is not affected by the geometry of the cladode.

The k_c values found are in the range of 0.0155 to 0.1366 g_{H2O} g_{db}^{-1} s^{-1} which are higher values than those reported by Zielinska *et al*. (2018) for osmo-microwave-vacuum drying of cranberries ranging from 1.050 $\times10^{-3}$ to 2.260$\times10^{-3}$ g_{H2O} g_{db}^{-1} s^{-1}, and those reported by Horuz, Bozkurt, Karata, and Maskan (2018) from 1.51$\times10^{-3}$ to 3.15$\times10^{-3}$ min^{-1} (2.52$\times10^{-5}$ a 5.52$\times10^{-5}$ s^{-1}) for combined hot air with microwave drying of apple slices. This difference in the order of magnitude is because the power density applied to the treatments in the literature is much lower than that reported in this work.

Table 4 shows the values obtained of drying constant k_{dec} for each treatment. Three groupings can be observed according to the diameter of each cladode (81.1±1.9, 112.2±4.7 and 126.1±2.6 mm respectively). The first group with a diameter of 81.1 mm was separated, while the groups with higher diameter are very close to each other. The value of k_{dec} in each group is directly proportional to the power density applied, showing a good agreement with

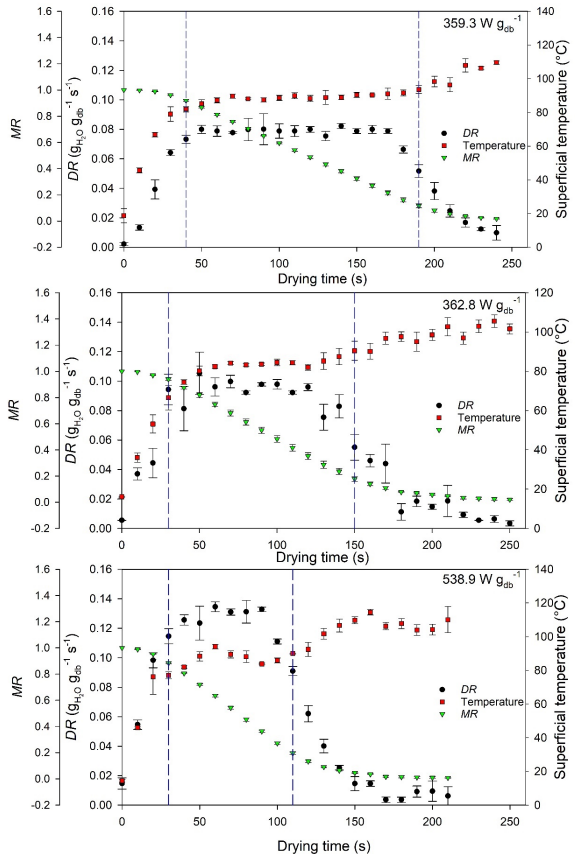

Figure 6. Drying curves of cactus cladodes at 359.3, 362.8 and 538.9 W g_{db}^{-1}.

linear fitting. The group with lower diameter value shows a lower slope, meanwhile higher diameter groups have higher slope. This means the diameter of the cladode influences the drying rate. The samples with largest diameter tend to be the thickest (Table 2); higher thick means higher area to mass transfer.

In the literature it can find values of k_{dec} for nopal drying using different methods. The values reported by Díaz-Ayala *et al.* (2015) for drying of thin slices of cladode with convective crossflow air were from 1.68 $\times 10^{-4}$ to 5.75$\times 10^{-4}$ s^{-1}; by Pereira *et al.* (2017) for drying prickly pear shoots with forced hot air reported values from 1.77 $\times 10^{-3}$ to 1.52 $\times 10^{-2}$ s^{-1}. Thus, it can be observed that the values found in this work are within the range found in the literature.

Like k_{dec}, plotting D_{eff} vs power density, three groups can be seen based on the average diameter of the treatments (Table 4). In each group, the D_{eff} value increased relative to the increase in applied energy density and sample diameter. This grouping is mostly differentiated because Equation 10 does consider the geometry of the cladode. With the energy densities applied, a maximum value of effective diffusivity was not reached. In future experiments, a higher D_{eff} value could be achieved by increasing the energy density in period III (however, sample deterioration by overheating could occur) or by choosing cladodes with a greater thickness and diameter. In period III the applied energy is less effective, so choosing suitable cladodes (longer and thicker) could produce energy savings in the process.

The D_{eff} values obtained were from 2.20$\times 10^{-6}$ a 5.59$\times 10^{-5}$ m^2 s^{-1}. These values are higher than those reported for drying nopal by different methods. For vacuum-dried nopal rectangles, effective diffusivity values of between 2.96 to 3.73$\times 10^{-7}$ m^2 s^{-1} were found and for forced convective drying in a temperature range of 40 to 60°C were from 3.99 to 5.35 $\times 10^{-7}$ m^2 s^{-1} (Dey *et al.*, 2019); from 8.32x10-12 to 1.30$\times 10^{-11}$ m^2 s^{-1} for osmotic drying of cladodes at different temperatures and °Brix (Medina-Torres *et al.*, 2008); from 1.77$\times 10^{-10}$ to 5.07$\times 10^{-10}$ m^2 s^{-1} for cladodes by infrared drying with temperatures from 40 to 60°C (Touil *et al.*, 2014). The results suggest that in phase III, microwave drying is faster than the reported methods, although it may affect the nutritional properties of nopal.

Table 3. Characteristics of cactus cladodes slabs during and after each microwave drying treatment.

Treatment (#)	Power density (W g_{db}^{-1})	Drying time (s)	a_w	Period II T_{avg} (ºC)	Period III $T_{\max}$ (ºC)	M_0 (g_{H2O} g_{db}^{-1})	M_{cr} (g_{H2O} g_{db}^{-1})	M_f (g_{H2O} g_{db}^{-1})
1	60.3	1550	0.43 ± 0.05	77.3±5.2	93	13.8 ± 0.58	1.6 ± 0.46	0.25±0.03
2	80.4	1300	0.42 ± 0.02	73.6±5.4	93	14.8 ± 0.20	2.9 ± 1.61	0.32±0.11
3	120.6	1010	0.41 ± 0.01	74.7±3.8	84	14.6 ± 0.10	2.6 ± 0.37	0.35±0.04
4	181.4	420	0.53 ± 0.09	84.8±4.4	114	14.3 ± 0.06	1.8 ± 0.31	0.47±0.04
5	241.9	360	0.47 ± 0.09	83.2±4.9	117	14.4 ± 0.10	2.4 ± 0.11	0.24±0.08
6	269.4	320	0.61 ± 0.10	90.9±3.6	116	14.1 ± 0.25	2.5 ± 1.05	1.13±0.39
7	359.3	260	0.47 ± 0.09	88.9±3.9	118	14.4 ± 0.13	1.9 ± 0.32	0.35±0.07
8	362.8	250	0.42 ± 0.01	82.2±7.2	99	14.7 ± 0.21	2.8 ± 0.44	0.46±0.27
9	538.9	220	0.43 ± 0.01	86.5±5.6	111	13.9 ± 0.13	3.1 ± 0.22	0.29±0.03

M_0= Initial moisture; M_f=Final moisture; M_{cr}: Critical moisture; a_w= water activity; T_{avg}=average temperature in period with constant rate drying; $T_{\max}$: Maximum temperature reached in falling period drying.

Table 4. Comparison of various parameters from each treatment of cladode slabs using microwave drying.

Treatment (#)	Power density (W g_{db}^{-1})	Diameter (mm)	Mean diameter of grouping (mm)	$k_{dec} \times 10^{-2}$ (s^{-1})	Slope of grouping ($g_{db}W^{-1}s^{-1}$)	$D_{eff} \times 10^{-7}$ (m^2s^{-1})	Slope of grouping (m^2 s^{-1} $g_{db}W^{-1}$)
3	120.6	80.0± 5.0		0.55±0.0001		0.173	
8	362.8	80.0± 0.0	81.1±1.9	2.31±0.0009	7.4×10^{-5}	1.268	5.27×10^{-8}
9	538.9	83.3± 2.9		3.65±0.0008	(R^2=0.9997)	1.747	(R^2=0.9915)
2	80.4	113.3± 5.8		0.58±0.0002		0.275	
5	241.9	116.7±11.5	112.2±4.7	2.61±0.0007		1.729	1.35×10^{-7}
7	359.3	107.5±3.5		3.75±0.0005	1×10^{-4}	1.910	(R^2 = 0.9356)
1	60.3	126.7±16.1		0.66±0.0002	(R^2=0.9351)	0.364	
4	181.4	123.3±7.6	126.1±2.6	2.44±0.0004		1.605	2.21×10^{-7}
6	269.4	128.3±7.6		3.35±0.0023		2.666	(R^2 =0.9959)

In comparison with others drying methods and materials; the values of D_{eff} reported ranged from 5.67×10^{-9} to 1.05×10^{-7} m^2 s^{-1} for Cecina using combined solar-convective drying (Tlatelpa-Becerro *et al*., 2022), and from 1.27×10^{-7} to 5.62×10^{-6} m^2 s^{-1} for Moroccan pomegranate arils using convective and greenhouse drying (El Broudi *et al*., 2022).

3.4 Cactus cladode drying modeling

Table 5 presents the parameter values of the fitting equations used (Sigmoid, Page and Rational) and their fitting (χ^2, RMSE, R^2). The fit equations presented quite acceptable adjustments; however, no model was fully adjusted to all treatments, nor to the complete drying process, in specific, in period changes. This can be a disadvantage if it is required to know or determine the critical humidity or the exact time where the periods begin. Because the fit of the model decreases when considering the complete drying process, for kinetics that present at least periods I and II it is recommended to model independently each period. In this work it was observed that Equation 7 is suitable for period II and Equations 8 or 10 for period III.

3.5 Superficial temperature

Period I was characterized by a faster temperature increase to a maximum. In period II, the temperature value was almost constant (T_{avg}, Table 3). The value of T_{avg} did not exceed 100°C, the maximum value obtained was 90.9±3.6°C. While in period III, in general an increase in temperature was observed. During this period, the temperature exceeded 100 °C in most treatments. Which can happen because the material contains less moisture, and it tends to be heated by the excess energy supplied (Zhang, Tang, Mujumdar, & Wang, 2006). Some treatments had to be suspended early to avoid carbonization or damage to the sample; such was the case for the last six energy densities. It is observed that treatments with lower energy densities (60.3, 80.4 and 120.6 W g_{db}^{-1}) presented a decrease in temperature at the end of period III even lower than the value of T_{avg}. This group also had low M_f values (Table 3). Consequently, these energy densities can be used in period III for microwave drying nopal cladodes to avoid high temperatures. The temperature behavior, observed in each period, was similar to that reported by different authors (Liu *et al*., 2019; Monteiro *et al*., 2020; Monteiro, Link, Tribuzi, Carciofi, & Laurindo, 2018; Qiu, Kloosterboer, Guo, Boom, & Schutyser, 2019). A recommendation to avoid overheating the sample in period III, is to adjust or control the power density so that it is possible to continue drying and avoid higher temperatures that cause burns and deterioration of vegetal material. In the literature it has been reported that, by controlling the power, in microwave drying, damage to the quality of the material is avoided (Luo *et al*., 2019; Monteiro *et al*., 2020) and products with lower moisture values are obtained.

3.6 Activation energy

By plotting of ln (D_{eff}) vs m_f P (g W^{-1}), a grouping of samples was observed according to the diameter (81.1±1.9, 112.2±4.7 and 126.1±2.6 mm). The coefficients of determination for each activation energy (22.08, 11.41 and 7.80 kW kg^{-1}) were 0.999, 1.000 and 0.994, ordered from lowest to largest diameter. The values of D_0 were -9.9836, -9.4984 and -9.3759, respectively. The activation energy shown a trend that was inversely proportional to the diameter, but directly proportional with thickness of sample.

The results obtained are consistent with what was reported by Süfer, Sezer, and Demir (2017), Azimi-Nejadian and Hoseini (2019) and Çinir and Süfer (2020) for the drying of onion, potato, and radish slices, respectively; where it was observed that the activation energy also shown a trend inversely proportional to thickness of samples. The activation energy is the energy needed for the water within the sample to begin to diffuse; high values mean that the water is more strongly linked to the structure of the material (Azimi-Nejadian & Hoseini, 2019).

The range of activation energy values found in this research was similar to those reported in the literature. Values of 7.90 and 45.60 W g^{-1} for convective and microwave drying of: onion slices (Demiray *et al*., 2017); 21.6 W g^{-1} for garlic puree (İlter *et al*., 2018); 6.88 W g^{-1} for apple slices (Tepe & Tepe, 2020); 2.77 to 10.61 W g^{-1} for radish slices (Çinir & Süfer, 2020), and 2.25-6.08 W g^{-1} for onion with and without brine (Süfer *et al*., 2017).

Table 5. Model constants and statistical parameters of intermittent microwave drying curves for nopal cladodes.

Model	Power Density ($W\ g_{db}^{-1}$)	Model Constants				$\chi 2$	RMSE	R^2
Sigmoid		a	b	c	k			
	60.3	-0.05±0.01	1.17±0.02	584.6±8.2	(3.9±0.1) x10^{-3}	(1.74±1.25) x10^{-3}	(3.95±1.55) x10^{-2}	0.986±0.042
	80.4	-0.05±0.02	1.21±0.05	479.1±14.0	(4.2±0.3) x10^{-3}	(4.08±3.27) x10^{-3}	(6.02±2.42) x10^{-2}	0.966±0.064
	120.6	0.01±0.00	1.11±0.01	266.3±2.31	(8.3±0.1) x10^{-3}	(2.96±1.80) x10^{-4}	(1.53±0.61) x10^{-2}	0.998±0.016
	181.4	-0.16±0.02	1.35±0.04	199.7±2.36	(1.0±0.0) x10^{-2}	(2.66±1.32) x10^{-4}	(1.55±0.43) x10^{-2}	0.998±0.016
	241.9	-0.06±0.01	1.19±0.02	142.8±1.50	(1.6±0.0) x10^{-2}	(2.52±0.59) x10^{-5}	(1.53±0.19) x10^{-2}	0.998±0.016
	269.4	-0.17±0.06	1.36±0.11	137.4±4.37	(1.4±0.2) x10^{-2}	(1.15±0.61) x10^{-3}	(3.19±0.82) x10^{-2}	0.990±0.033
	359.3	-0.10±0.02	1.25±0.04	113.1±1.59	(1.9±0.1) x10^{-2}	(3.51±0.98) x10^{-4}	(1.78±0.27) x10^{-2}	0.997±0.019
	362.8	(8±0.9) x10^{-4}	1.11±0.03	88.9±1.77	(2.7±0.1) x10^{-2}	(6.63±4.41) x10^{-4}	(2.34±0.98) x10^{-2}	0.995±0.025
	538.9	-0.02±0.01	1.12±0.02	70.3±0.78	(3.6±0.1) x10^{-2}	(2.08±0.93) x10^{-4}	(1.33±0.32) x10^{-2}	0.998±0.014
Page		n	k					
	60.3	2.04±0.03	(1.48±0.26) x10^{-2}			(1.99±1.36) x10^{-3}	(4.25±1.54) x10^{-2}	0.984±0.044
	80.4	1.92±0.04	(4.24±1.05) x10^{-6}			(4.25±3.34) x10^{-3}	(6.16±2.42) x10^{-2}	0.965±0.065
	120.6	1.82±0.01	2.24±0.17) x10^{-6}			(3.48±1.68) x10^{-4}	(1.81±0.46) x10^{-3}	0.997±0.019
	181.4	2.08±0.03	(1.14±0.17) x10^{-5}			(5.89±0.82) x10^{-4}	(2.36±0.17) x10^{-2}	0.995±0.024
	241.9	2.05±0.03	(2.39±0.30) x10^{-5}			(4.34±1.37) x10^{-4}	(2.01±0.34) x10^{-2}	0.997±0.020
	269.4	2.06±0.05	(2.71±0.67) x10^{-5}			(1.36±0.60) x10^{-3}	(3.49±0.77) x10^{-2}	0.988±0.036
	359.3	2.11±0.04	(3.16±0.54) x10^{-5}			(6.02±1.83) x10^{-4}	(2.33±0.36) x10^{-2}	0.995±0.024
	362.8	1.96±0.03	(9.02±1.48) x10^{-5}			(6.49±4.55) x10^{-4}	(2.30±1.02) x10^{-2}	0.995±0.025
	538.9	2.07±0.03	(9.57±1.08) x10^{-5}			(2.26±1.21) x10^{-4}	(1.37±0.43) x10^{-2}	0.998±0.014
Rational		a	b	c	d			
	60.3	0.996±0.01	(-7.0±0.11) x10^{-4}	(-6.0±0.52) x10^{-4}	(1.3±0.08) x10^{-6}	(2.26±0.92) x10^{-3}	(4.66±0.92) x10^{-2}	0.985±0.044
	80.4	1.003±0.01	(-9.0±0.23) x10^{-4}	(-6.0±1.0) x10^{-4}	(1.6±0.19) x10^{-6}	(4.53±5.76) x10^{-3}	(5.79±4.08) x10^{-2}	0.966±0.064
	120.6	0.977±0.01	(-1.1±0.02) x10^{-3}	(-1.4±0.09) x10^{-3}	(9.0±0.33) x10^{-6}	(6.21±2.30) x10^{-4}	(2.44±0.48) x10^{-2}	0.995±0.025
	181.4	1.019±0.01	(-2.6±0.02) x10^{-3}	(-1.6±0.09) x10^{-3}	(7.7±0.50) x10^{-6}	(2.53±1.28) x10^{-4}	(1.51±0.42) x10^{-2}	0.998±0.015
	241.9	1.004±0.01	(-3.1±0.04) x10^{-3}	(-2.5±0.20) x10^{-3}	(2.1±0.11) x10^{-5}	(3.55±0.36) x10^{-4}	(1.83±0.01) x10^{-2}	0.997±0.018
	269.4	1.021±0.01	(-3.7±0.10) x10^{-3}	(-2.3±0.30) x10^{-3}	(1.6±0.29) x10^{-5}	(1.11±0.39) x10^{-3}	(3.17±0.54) x10^{-2}	0.990±0.033
	359.3	1.012±0.01	(-4.3±0.06) x10^{-3}	(-3.1±0.20) x10^{-3}	(3.0±0.22) x10^{-5}	(3.63±1.12) x10^{-4}	(1.81±0.28) x10^{-2}	0.997±0.019
	362.8	0.994±0.01	(-4.1±0.10) x10^{-3}	(-4.5±0.50) x10^{-3}	(7.3±0.59) x10^{-5}	(7.97±5.07) x10^{-4}	(2.61±0.92) x10^{-2}	0.994±0.028
	538.9	0.998±0.01	(-6.1±0.10) x10^{-3}	(-5.9±0.40) x10^{-3}	(1.0±0.07) x10^{-4}	(3.25±0.06) x10^{-1}	(5.35±0.05) x10^{-1}	0.998±0.017

Conclusions

Kinetics of drying nopal cladode, with different energy densities, were characterized. All drying kinetics showed three periods: heating (I), constant drying rate (II) and falling drying rate (III). In this drying process, the water migrates from the inside to the outside along the sides of the cladode, where the lack of cuticle produces less resistance to its diffusion. In period II, the drying rate was directly proportional to the energy density applied. In period III, the diameter and thickness of the cladode influence the drying rate and the effective diffusivity. In addition, the activation energy is inversely related to the diameter and thickness of the cladode. For the microwave drying of nopal, it is recommended to use cladodes of greater thickness and diameter (usually those of greater age) of to lead the drying rate and the effective diffusivity more efficiently in period III, since in this period the energy applied is less effective. In addition, to avoid overheating in period III, surface temperature could be modulated using power density control.

Nomenclature

P	power (W)
m_1	mass of water heated (g)
m_2	mass of water evaporated (g)
Cp_{H2O}	heat capacity of water (J °C^{-1} g$^{-1}_{H2O}$)
ΔT	increase of temperature (°C)
λ	heat of vaporization of water (J g$^{-1}_{H2O}$)
t_{on}	time of microwave heating (s)
PR	pulse ratio
t_{off}	time without treatment (s)
a_w	water activity
M_t	moisture content (g$_{H2O}$ g^{-1}_{db})
m_{db}	mass of sample in dry basis (g$_{db}$)
m_{wb}	mass of the cladode (g$_{wb}$)
MR	moisture ratio
M_t	moisture content of sample at the time I (g$_{H2O}$ g^{-1}_{db})
M_0	initial moisture content of the sample (g$_{H2O}$ g^{-1}_{db})
DR	drying rate (g$_{H2O}$ g$^{-1}_{db}$ s^{-1})
ΔM_t	(g$_{H2O}$ g^{-1}_{db}) change in moisture during the drying treatment period
M_{cr}	critical moisture (g$_{H2O}$ g^{-1}_{db})
$M_{0,cr}$	moisture where the constant drying rate period begins
k_c	constant drying rate (g$_{H2O}$ g^{-1}_{db} s^{-1})
k_1	is the quadratic constant (g$_{H2O}$ g^{-1}_{db} s^{-1})
t$_{0.cr}$	time at constant drying rate period begins (s)
t$_{cr}$	time at constant drying rate period ends (s)
$M_{t,dec}$	moisture in the falling drying rate period (g$_{H2O}$ g^{-1}_{db})
k_{dec}	drying rate in the falling drying rate period (s^{-1})
D_{eff}	effective diffusivity (m^2 s^{-1})
MR_{dec}	moisture ratio in the decreasing period (g$_{H2O}$ g^{-1}_{db})
L	half the thickness of the slab before drying process (m)
D_0	preexponential factor (m^2 s^{-1})
E_a	activation energy (W g^{-1})
m_f	fresh mass of sample before treatment (g)
R^2	coefficient of determination
χ^2	chi square
RMSE	root of the mean square error

References

Aruwa, C. E., Amoo, S. O., & Kudanga, T. (2018). *Opuntia* (Cactaceae) plant compounds, biological activities and prospects - A comprehensive review. *Food Research International 112*, 328-344. https://doi.org/10.1016/j.foodres.2018.06.047

Azimi-Nejadian, H., & Hoseini, S. S. (2019). Study the effect of microwave power and slices thickness on drying characteristics of potato. *Heat and Mass Transfer 55*(10), 2921-2930. https://doi.org/10.1007/s00231-019-02633-x

Barba, F. J., Garcia, C., Fessard, A., Munekata, P. E. S., Lorenzo, J. M., Aboudia, A., Remize, F. (2020). *Opuntia Ficus Indica* Edible Parts: A Food and Nutritional Security Perspective. *Food Reviews International*, 1-23. https://doi.org/10.1080/87559129.2020.1756844

Barreto, I. M. A., Tribuzi, G., Marsaioli Junior, A., Carciofi, B. A. M., & Laurindo, J. B. (2019). Oil-free potato chips produced by microwave multiflash drying. *Journal of Food Engineering 261*, 133-139. https://doi.org/10.1016/j.jfoodeng.2019.05.033

Briki, S., Zitouni, B., Bechaa, B., & Amiali, M. (2019). Comparison of convective and infrared heating as means of drying pomegranate arils (*Punica granatum* L.). *Heat and Mass Transfer 55*(11), 3189-3199. https://doi.org/10.1007/s00231-019-02644-8

Chandrasekaran, S., Ramanathan, S., & Basak, T. (2013). Microwave food processing-A review. *Food Research International 52*(1), 243-261. https://doi.org/10.1016/j.foodres.2013.02.033

Çinir, N. *İ*., & Süfer, Ö. (2020). Microwave drying of TURKISH red meat (watermelon) radish (*Raphanus sativus* L.): effect of osmotic dehydration, pre-treatment and slice thickness. *Heat and Mass Transfer 56*(12), 3303-3313. https://doi.org/10.1007/s00231-020-02930-w

Cruz-de la Cruz, L. L., Espinosa-Solares, T., Aguilar-Méndez, M. A., Guerra-Ramírez, D., & Hernández-Eugenio, G. (2020). Influence of microwave drying process on microstructure and thermodynamic properties of nopal cladodes. *Ingeniería Agrícola y Biosistemas 12*(2), 115-130. https://doi.org/10.5154/r.inagbi.2019.12.075www.chapingo.mx/revistas/inagbi

Dadali, G., & Özbek, B. (2008). Microwave heat treatment of leek: drying kinetic and effective moisture diffusivity. *International Journal of Food Science & Technology 43*(8), 1443-1451. https://doi.org/10.1111/j.1365-2621.2007.01688.x

Dai, J.-W., Xiao, H.-W., Zhang, L.-H., Chu, M.-Y., Qin, W., Wu, Z.-J., Han, D.-D., Li, Y.-L., Liu, Y.-W., Yin, P.-F. (2019). Drying characteristics and modeling of apple slices during microwave intermittent drying. *Journal of Food Process Engineering 42*(6), e13212. https://doi.org/10.1111/jfpe.13212

Dehghannya, J., Bozorghi, S., & Heshmati, M. K. (2018). Low temperature hot air drying of potato cubes subjected to osmotic dehydration and intermittent

microwave: drying kinetics, energy consumption and product quality indexes. *Heat and Mass Transfer 54*(4), 929-954. https://doi.org/10.1007/s00231-017-2202-5

Demiray, E., Seker, A., & Tulek, Y. (2017). Drying kinetics of onion (*Allium cepa* L.) slices with convective and microwave drying. *Heat and Mass Transfer 53*(5), 1817-1827. https://doi.org/10.1007/s00231-016-1943-x

Dey, A., Singhal, S., Rasane, P., Kaur, S., Kaur, N., & Singh, J. (2019). Comparative kinetic analysis of convective and vacuum dried *Opuntia ficus-indica* (L.) Mill. cladodes. *Research in Agricultural Engineering 65*(1), 1-6. https://doi.org/10.17221/18/2018-RAE

Díaz-Ayala, F., Álvarez-García, G. d. S., & Simá-Moo, E. (2015). Drying kinetics of slices of nopal (*Opuntia ficus indica*) cladodes in a convective transversal flow dryer. *Agrociencia 49*, 845-857. Retrieved from http://www.scielo.org.mx/scielo.php?script=sci_arttext&pid=S1405-31952015000800003&nrm=iso

Dong, H., Dai, T., Liang, L., Deng, L., Liu, C., Li, Q., Liang, R., Chen, J. (2021). Physicochemical properties of pectin extracted from navel orange peel dried by vacuum microwave. *LWT 151*, 112100. https://doi.org/10.1016/j.lwt.2021.112100

El-Mostafa, K., El Kharrassi, Y., Badreddine, A., Andreoletti, P., Vamecq, J., El Kebbaj, M., Hammed, S., Latruffe, N., Lizard, G., Nasser, B., Cherkaoui-Malki, M. (2014). Nopal Cactus (*Opuntia ficus-indica*) as a Source of Bioactive Compounds for Nutrition, Health and Disease. *Molecules 19*(9), 14879-14901. https://doi.org/10.3390/molecules190914879

El Broudi, S., Zehhar, N., Abdenouri, N., Boussaid, A., Hafidi, A., Bouamama, H., & Benkhalti, F. (2022). Investigation of drying kinetics and drying conditions on biochemical, sensory, and microstructural parameters of "Sefri" pomegranate arils (*Punica granatum* L. a Moroccan variety). *Revista Mexicana de Ingeniería Química 21*(3), Alim2813. https://doi.org/10.24275/rmiq/Alim2813

García-Valladares, O., Cesar-Munguía, A. L., López-Vidaña, E. C., Castillo-Téllez, B., Ortíz-Sánchez, C. A., Lizama-Tzec, F. I., & Domínguez-Niño, A. (2022). Effect by using a modified solar dryer on physicochemical properties of carambola fruit (*Averrhoa Carambola* L.). *Revista Mexicana de Ingeniería Química 21*(1), Alim2650. https://doi.org/10.24275/rmiq/Alim2650

Horuz, E., Bozkurt, H., Karataş, H., & Maskan, M. (2018). Simultaneous application of microwave energy and hot air to whole drying process of apple slices: drying kinetics, modeling, temperature profile and energy aspect. *Heat and Mass Transfer 54*(2), 425-436. https://doi.org/10.1007/s00231-017-2152-y

İlter, I., Akyil, S., Devseren, E., Okut, D., Koç, M., & Kaymak Ertekin, F. (2018). Microwave and hot air drying of garlic puree: drying kinetics and quality characteristics. *Heat and Mass Transfer 54*(7), 2101-2112. https://doi.org/10.1007/s00231-018-2294-6

Inglese, P., Mondragon Jacobo, C., Nefzaoui, A., & Sáenz, C. (Eds.). (2018). *Ecologia del cultivo, manejo y usos del nopal*. Roma: Food and Agriculture Organization of the United Nations (FAO).

Jebri, M., Desmorieux, H., Maaloul, A., Saadaoui, E., & Romdhane, M. (2019). Drying of *Salvia officinalis* L. by hot air and microwaves: dynamic desorption isotherms, drying kinetics and biochemical quality. *Heat and Mass Transfer 55*(4), 1143-1153. https://doi.org/10.1007/s00231-018-2498-9

Karimi, S., Layeghinia, N., & Abbasi, H. (2021). Microwave pretreatment followed by associated microwave-hot air drying of *Gundelia tournefortii* L.: drying kinetics, energy consumption and quality characteristics. *Heat and Mass Transfer 57*(1), 133-146. https://doi.org/10.1007/s00231-020-02948-0

Liu, C., Grimi, N., Lebovka, N., & Vorobiev, E. (2019). Convective air, microwave, and combined drying of potato pre-treated by pulsed electric fields. *Drying Technology 37*(13), 1704-1713. https://doi.org/10.1080/07373937.2018.1536065

López, R., de Ita, A., & Vaca, M. (2009). Drying of prickly pear cactus cladodes (*Opuntia ficus indica*) in a forced convection tunnel. *Energy Conversion and Management 50*(9), 2119-2126. https://doi.org/10.1016/j.enconman.2009.04.014

Luo, G., Song, C., Hongjie, P., Li, Z., Xu, W., Raghavan, G. S. V., Jin, G. (2019). Optimization of the microwave drying process for potato chips based on the measurement of dielectric properties. *Drying Technology 37*(11), 1329-1339. https://doi.org/10.1080/07373937.2018.1500482

Medina-Torres, L., Gallegos-Infante, J. A., Gonzalez-Laredo, R. F., & Rocha-Guzman, N. E. (2008). Drying kinetics of nopal (*Opuntia ficus-indica*) using three different methods and their effect on their mechanical properties. *LWT - Food Science and Technology 41*(7), 1183-1188. https://doi.org/10.1016/j.lwt.2007.07.016

Monteiro, R. L., Gomide, A. I., Link, J. V., Carciofi, B. A. M., & Laurindo, J. B. (2020). Microwave vacuum drying of foods with temperature control by power

modulation. *Innovative Food Science & Emerging Technologies 65*, 102473. https://doi.org/10.1016/j.ifset.2020.102473

Monteiro, R. L., Link, J. V., Tribuzi, G., Carciofi, B. A. M., & Laurindo, J. B. (2018). Microwave vacuum drying and multi-flash drying of pumpkin slices. *Journal of Food Engineering 232*, 1-10. https://doi.org/10.1016/j.jfoodeng.2018.03.015

Pereira, E., Silva, W., Gomes, J., Da, C., Silva, S., Dos, A., Costa, F. (2017). Empirical models in the description of prickly pear shoot (Nopal) drying kinetics. *Revista Brasileira de Engenharia Agrícola e Ambiental 21*, 798. https://doi.org/10.1590/1807-1929/agriambi.v21n11p798-802

Perucini-Avendaño, M., Nicolás-García, M., Jiménez-Martínez, C., Perea-Flores, M. d. J., Gómez-Patiño, M. B., Arrieta-Báez, D., & Dávila-Ortiz, G. (2021). Cladodes: Chemical and structural properties, biological activity, and polyphenols profile. *Food Science & Nutrition 9*(7), 4007-4017. https://doi.org/10.1002/fsn3.2388

Qiu, J., Kloosterboer, K., Guo, Y., Boom, R. M., & Schutyser, M. A. I. (2019). Conductive thin film drying kinetics relevant to drum drying. *Journal of Food Engineering 242*, 68-75. https://doi.org/10.1016/j.jfoodeng.2018.08.021

Quintero-García, M., Gutiérrez-Cortez, E., Bah, M., Rojas-Molina, A., Cornejo-Villegas, M. d. l. A., Del Real, A., & Rojas-Molina, I. (2021). Comparative Analysis of the Chemical Composition and Physicochemical Properties of the Mucilage Extracted from Fresh and Dehydrated *Opuntia ficus indica* Cladodes. *Foods 10*(9), 2137. Retrieved from https://www.mdpi.com/2304-8158/10/9/2137

Ramadan, M. F., Moussa Ayoub, T. E., & Rohn, S. (2021). Introduction to Opuntia spp.: Chemistry, Bioactivity and Industrial Applications. In M. F. Ramadan, T. E. M. Ayoub, & S. Rohn (Eds.), *Opuntia spp.: Chemistry, Bioactivity and Industrial Applications* (pp. 3-11). Cham: Springer International Publishing.

Rattanadecho, P., & Makul, N. (2016). Microwave-Assisted Drying: A Review of the State-of-the-Art. *Drying Technology 34*(1), 1-38. https://doi.org/10.1080/07373937.2014.957764

SADER. (2020). Crece en México el consumo y producción de nopal: Agricultura [Press release]. Retrieved from https://www.gob.mx/agricultura/prensa/crece-en-mexico-el-consumo-y-produccion-de-nopal-agricultura?idiom=es

Sáenz, C., & Berger, H. (2006). *Utilización agroindustrial del nopal*: FAO.

Shafiur-Rahman, M. (2020). Food Preservation: An Overview. In F. P. A. Overview (Ed.), (3rd ed., pp. 12). *Handbook of Food Preservation*. CRC Press.

Shu, B., Wu, G., Wang, Z., Wang, J., Huang, F., Dong, L., Su, D. (2020). The effect of microwave vacuum drying process on citrus: drying kinetics, physicochemical composition and antioxidant activity of dried citrus (*Citrus reticulata Blanco*) peel. *Journal of Food Measurement and Characterization 14*(5), 2443-2452. https://doi.org/10.1007/s11694-020-00492-3

SIAP. (2021). Anuario Estadístico de la Producción Agrícola. Retrieved from https://nube.siap.gob.mx/cierreagricola/. Retrieved Dec/18th/2021, from Servicio de Información Agroalimentaria y Pesquera. Gobierno de México https://nube.siap.gob.mx/cierreagricola/

Siebert, T., Gall, V., Karbstein, H. P., & Gaukel, V. (2018). Serial combination drying processes: A measure to improve quality of dried carrot disks and to reduce drying time. *Drying Technology 36*(13), 1578-1591. https://doi.org/10.1080/07373937.2017.1418374

Süfer, Ö., Sezer, S., & Demir, H. (2017). Thin layer mathematical modeling of convective, vacuum and microwave drying of intact and brined onion slices. *Journal of Food Processing and Preservation 41*(6), e13239. https://doi.org/10.1111/jfpp.13239

Surendhar, A., Sivasubramanian, V., Vidhyeswari, D., & Deepanraj, B. (2019). Energy and exergy analysis, drying kinetics, modeling and quality parameters of microwave-dried turmeric slices. *Journal of Thermal Analysis and Calorimetry 136*(1), 185-197. https://doi.org/10.1007/s10973-018-7791-9

Tepe, T. K., & Tepe, B. (2020). The comparison of drying and rehydration characteristics of intermittent-microwave and hot-air dried-apple slices. *Heat and Mass Transfer 56*(11), 3047-3057. https://doi.org/10.1007/s00231-020-02907-9

Tlatelpa-Becerro, A., Rico-Martínez, R., Cárdenas-Manríquez, M., Urquiza, G., Castro-Gómez, L., Alarcón-Hernández, F., Montiel, E. (2022). Drying kinetics of Cecina from Yecapixtla using a forced flow indirect solar dryer. *Revista Mexicana de Ingeniería Química 21*(3), Alim2813. https://doi.org/10.24275/rmiq/Alim2750

Torres Salcido, J. G., & Cornejo Oviedo, F. M. (2018). Organización y liderazgo en la construcción de un Sistema Agroalimentario Localizado. Un estudio de caso sobre el nopal en Hidalgo, México. *Estudios sociales (Hermosillo, Son.)*, 28, 0-0. https://doi.org/10.24836/es.v28i51.496

Touil, A., Chemkhi, S., & Zagrouba, F. (2014). Moisture Diffusivity and Shrinkage of Fruit and Cladode of *Opuntia ficus-indica* during Infrared Drying. *Journal of Food Processing 2014*, 175402. https://doi.org/10.1155/2014/175402

Turkmen, F., Karasu, S., & Karadag, A. (2020). Effects of Different Drying Methods and Temperature on the Drying Behavior and Quality Attributes of Cherry Laurel Fruit. *Processes 8*(7), 761. Retrieved from https://www.mdpi.com/2227-9717/8/7/761

Ventura-Aguilar, R. I., Bosquez-Molina, E., Bautista-Baños, S., & Rivera-Cabrera, F. (2017). Cactus stem (*Opuntia ficus-indica* Mill): anatomy, physiology and chemical composition with emphasis on its biofunctional properties. *Journal of the Science of Food and Agriculture 97*(15), 5065-5073. https://doi.org/10.1002/jsfa.8493

Zhang, M., Tang, J., Mujumdar, A. S., & Wang, S. (2006). Trends in microwave-related drying of fruits and vegetables. *Trends in Food Science & Technology 17*(10), 524-534. https://doi.org/10.1016/j.tifs.2006.04.011

Zhu, A., & Shen, X. (2014). The model and mass transfer characteristics of convection drying of peach slices. *International Journal of Heat and Mass Transfer 72*, 345-351. https://doi.org/10.1016/j.ijheatmasstransfer.2014.01.001

Zielinska, M., Zielinska, D., & Markowski, M. (2018). The Effect of Microwave-Vacuum Pretreatment on the Drying Kinetics, Color and the Content of Bioactive Compounds in Osmo-Microwave-Vacuum Dried Cranberries (*Vaccinium macrocarpon*). *Food and Bioprocess Technology 11*(3), 585-602. https://doi.org/10.1007/s11947-017-2034-9